Fragility Analysis of Pangasinan State University Urdaneta City Campus Buildings

RUTH ANN D. MANINGDING[1,*], JAN NICHOLAS S. BALDO[2]
[1]College of Engineering and Architecture,
Pangasinan State University,
Urdaneta City, Pangasinan, 2428,
PHILIPPINES

[2]College of Engineering and Architecture,
University of Cordilleras,
Baguio City, Benguet, 2600,
PHILIPPINES

Corresponding Author

Abstract: – The Philippines is a seismically susceptible region because of its unique geographical location within the Pacific Ring of Fire. Over the years, the Philippines has had several destructive earthquakes that have caused building collapses and numerous fatalities. Schools are particularly vulnerable to earthquakes because most were built using outdated building rules that do not comply with current seismic design criteria. The age of PSU buildings, which ranges from 10 to 40 years, may increase their vulnerability to seismic hazards. Buildings designed with the old codes might lack the necessary reinforcement and structural elements to withstand the forces generated by an earthquake, potentially leading to catastrophic failures and endangering the lives of students, faculty, and other occupants. Moreover, the San Manuel Fault Line near PSU buildings in Urdaneta City, Pangasinan, heightens the risk of a significant seismic event affecting these structures. Given the critical role that schools play in communities, both in providing education and serving as essential facilities during and after disasters, assessing their seismic vulnerability becomes crucial. So far, no research has been conducted to evaluate the PSU building's vulnerability to seismic activity in the event of a significant earthquake. In line with this, this study aimed to perform a seismic fragility analysis of PSU buildings in Urdaneta City, Pangasinan, Philippines, to determine how susceptible they were to earthquakes. This study applies preliminary assessment using Rapid Visual Screening of FEMA P-154 to filter out which buildings need further evaluation and detailed assessment using fragility analysis. The screened buildings are evaluated using fragility curves to assess if the building could endure an earthquake with a 0.4 g PGA and a 10% probability of exceedance, following the National Structural Code of the Philippines (NSCP) requirements for seismic zone 4. The structural model of PSU buildings was created using SAP 2000, and the non-linear static analysis, specifically the ATC40 Capacity Spectrum Method, was performed to determine the data required to develop the fragility curves. The results demonstrate that the seismic scores of Engineering Buildings 1, 2, and 3 are below the RVS FEMA P-154 standard of 2.0, indicating that further investigation is required to evaluate their vulnerability thoroughly. Additionally, these buildings were observed to withstand a maximum peak ground acceleration of 0.60 g PGA at a 10% probability of exceedance based on the developed fragility curves, corresponding to earthquake intensity up to VIII, indicating "severe shaking." Furthermore, analysis of the fragility curves demonstrates that none of the structures exceed the 10% probability of exceedance at 0.4 g PGA, aligning with NSCP standards for Seismic Zone 4. As a result, these buildings are considered safe for occupancy without requiring retrofitting measures.

Key-Words: - earthquake, rapid visual survey, seismic vulnerability assessment, fragility analysis, capacity spectrum method, probability of exceedance.

Received: June 13, 2024. Revised: October 25, 2024. Accepted: November 21, 2024. Published: December 12, 2024.

1 Introduction

1.1 Background of the Study

Earthquakes can occur unexpectedly and without warning, [1]. When tectonic plates move along a fault line in the crust of the earth, it can generate intense shaking of the ground, which is known as an earthquake, [2]. The Philippines is prone to seismic activity due to its distinctive geographic position within the Pacific Ring of Fire. Over time, the nation has experienced devastating earthquakes, resulting in building failures and significant loss of life, [3].

Schools are particularly vulnerable to earthquakes because most were built using outdated building rules that do not comply with current seismic design criteria, and others were constructed without seismic design. Despite the inclusion of seismic provisions in modern construction, older buildings might still pose risks to occupants due to their age and deterioration, [4], [5]. The seismic vulnerability assessment of schools needs special attention due to its essential role in the community, both in education and post-earthquake function. Schools play a valuable additional role in disaster recovery efforts. When there is an emergency, schools are usually utilized as evacuation centers, [6]. The Department of Education in the Philippines has designated schools as evacuation centers, ensuring they are readily available during disasters, [7]. During emergencies, a more secure and resilient school may save children's lives and help get things back to normal in the community, [8].

Due to its location close to the San Manuel Fault Line, PSU buildings will be affected by a significant seismic event. The San Manuel fault line is 12.7 kilometers away from the structures, according to the Phivolcs Fault Finder App, [9]. Moreover, the age range of most PSU buildings is 10 to 40 years old. The age of the structures may contribute to their susceptibility to earthquake hazards. The structural reliability and integrity of the buildings may decrease over time due to normal wear and tear, environmental conditions, and structural deterioration, [10]. These structures were designed and built using outdated building codes that fail to meet current seismic design standards.

This study analyzed the seismic fragility of PSU buildings in Urdaneta City, Pangasinan, Philippines, to determine their susceptibility to earthquakes. It applied preliminary assessment using Rapid Visual Screening and detailed assessment using fragility analysis of the buildings. Rapid Visual Screening (RVS) of FEMA P-154 provides an initial assessment of the buildings against earthquake hazards to filter out which buildings need further evaluation. The seismic susceptibility of the screened structures is evaluated using fragility curves, which depict the likelihood of collapse or damage at different levels of ground shaking.

One of the primary distinctions of this study is its specific focus on PSU Urdaneta City Campus Buildings. By developing fragility models that are tailored to the unique construction practices, materials, geological conditions, and environmental factors of Urdaneta City, this research directly addresses the specific needs of the region. This localization means that the findings directly apply to the city's specific context, making them highly relevant for local stakeholders, including city planners, engineers, policymakers, and school administration. They can use these precise insights to develop more effective mitigation strategies and improve the overall seismic resilience of PSU Urdaneta City Campus buildings and other public buildings within the region.

1.2 Objectives of the Study

This study was conducted to carry out a fragility analysis of PSU buildings in Urdaneta City, Pangasinan, Philippines, to evaluate their susceptibility to earthquake damage. Specifically:

1. To identify those buildings that need to be prioritized for further detailed seismic evaluation based on the cut-off score of FEMA P-154.
2. To determine the damage level of the selected PSU buildings when subjected to a peak ground acceleration of 0.4 g.
3. To obtain the seismic vulnerability of the selected PSU buildings based on the developed fragility curves.
4. To determine the maximum possible intensity that PSU buildings can withstand.

1.3 Conceptual Framework

The conceptual framework for this study applies a preliminary and detailed assessment of the buildings, as depicted in Figure 1. Rapid Visual Screening (RVS) is one of the valuable techniques for rapidly determining the seismic risk of significant structures, such as school buildings. These procedures will initially assess a building's vulnerability to seismic hazards. The buildings that have undergone screening with scores less than the cut-off of RVS FEMA P-154 are assessed for seismic vulnerability using fragility analysis, which shows the likelihood of failure or damage at various intensities of ground shaking.

Fig. 1: Conceptual Framework

1.4 Scope and Delimitation

The study focuses on conducting a fragility analysis of PSU buildings in Urdaneta City, Pangasinan, Philippines. The Rapid Visual Screening (RVS) method from FEMA P-154 prioritizes buildings and identifies those requiring additional evaluation. The PSU Urdaneta Campus has eleven (11) buildings considered for the study, as presented in Table 3. Actual measurements were conducted to verify the plans' dimensions, and the rebound hammer test was performed to assess the on-site compressive strength of the concrete. Also, to ensure accurate data for generating the fragility curves, the researchers conducted additional tests, including a tensile test, to determine the actual tensile strength of the rebars. This approach differentiates this study from others that rely solely on the specifications provided in the plans. The exposed rebars at the top of columns were acquired, and a tensile test was done using the Universal Testing Machine (UTM) on steel bars to assess the tensile strength of reinforcing bars.

SAP 2000 will create and simulate structure models subject to earthquakes. The major structural elements of the building are all included in the structural modeling, which is limited only by the concrete works. Microsoft Excel will run the simulation, analyze the results, and produce the fragility curves using the data collected. Nonlinear static "pushover" analysis will be carried out to generate capacity curves. The pushover parameters will follow the provisions of the ATC-40 Capacity Spectrum Method (CSM). The Incorporated Research Institutions for Seismology (IRIS) databases were used to collect the ground motion data (GMD). The structural models were subjected to seven (7) local earthquakes and five (5) international earthquakes. The seven (7) earthquakes that were recorded in the Philippines from 1988 to 2023 are displayed in Table 1 (Appendix). The five (5) earthquakes that occurred in foreign countries from 1996 to 2023 are presented in Table 2 (Appendix).

2 Methodology

The descriptive analytical case study method is selected to align with the necessary methodology, blending descriptive and analytical approaches to assess the building's susceptibility to seismic events thoroughly. A descriptive approach was employed for the preliminary assessment of the PSU buildings using Rapid Visual Survey forms. The analytical component evaluated the building's structural behavior and response to seismic events. A computational model of the PSU buildings was created using SAP 2000 software, and non-linear static analysis, specifically the ATC40 Capacity Spectrum Method, was performed to determine the data required to generate the fragility curves. These models simulated the building's response to seismic forces and helped assess its vulnerability and potential damage.

2.1 Research Design

Figure 2 is an illustration of the proposed procedure. PSU buildings will undergo a preliminary assessment utilizing Rapid Visual Screening to determine whether buildings require additional investigation. The obtained structural plan will be modeled using SAP 2000 software, and pushover analysis and response spectrum analysis will be carried out using the ground motion data gathered.

Pushover curves and response spectra, in turn, determine an earthquake's demand and a building's capacity. These first two components serve as inputs for the Capacity Spectrum Method used in structural assessments. Creating a fragility curve includes statistical analysis of the structural response data.

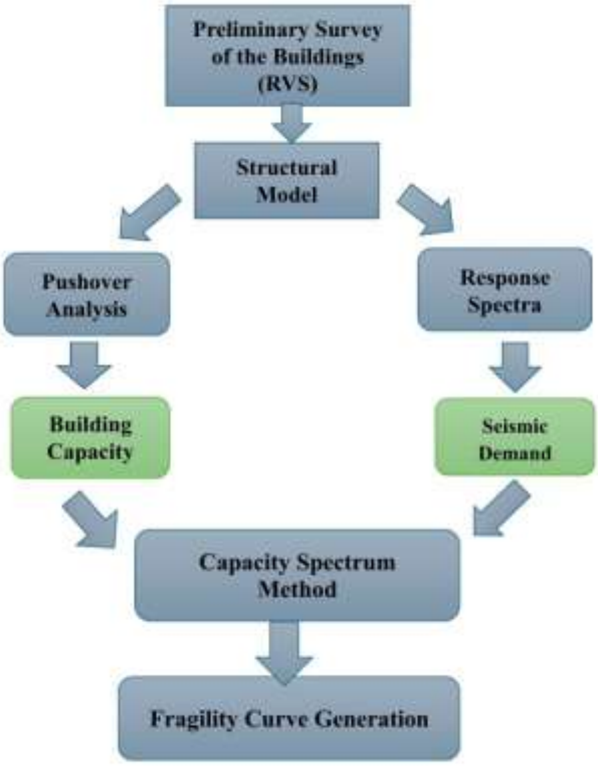

Fig. 2: Research Design

2.2 Population and Locale of the Study

The PSU Urdaneta City Campus is located along McArthur Highway in Barangay San Vicente, Urdaneta City, Pangasinan, Philippines, covering an area of 25,499 square meters. The city's precise geographical position is 15.9835° N latitude and 120.6334° E longitude. Figure 3 depicts the PSU Urdaneta Campus' site development plan. Eleven (11) school buildings, including the Graduate School building, were involved in the case study. The 11 buildings included in the study are listed in Table 3.

Fig. 3: PSU Urdaneta City Campus Site Development Plan

Table 3. Name of buildings in PSU Urdaneta City Campus

Building Number	Building Name
BLDG 1	Academic Building 1
BLDG 2	Academic Building 2
BLDG 3	Academic Building 2 (extension)
BLDG 4	Engineering Building 1
BLDG 5	Engineering Building 2
BLDG 6	Engineering Building 3
BLDG 7	Educational Building
BLDG 8	General Education Building
BLDG 9	PTBI (Pangasinan Technology Business Incubator Center)
BLDG 10	School of Advanced Studies
BLDG 11	Student Activity Center

2.3 Data Gathering Procedure

This study aims to create analytical fragility curves for the buildings at Pangasinan State University (PSU) Urdaneta Campus using a four-phase technique indicated in Figure 4.

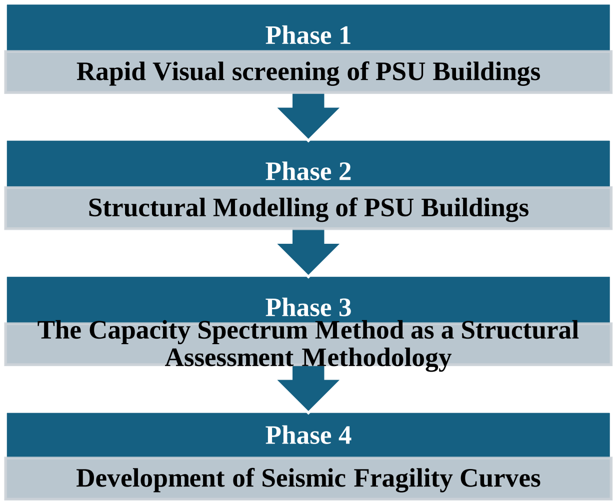

Fig. 4: Flow of Activity

2.3.1 Phase 1: Rapid Visual Screening (RVS)

Rapid Visual Screening (RVS) is an initial filter to identify buildings with potential seismic vulnerabilities, allowing for further evaluation and prioritization of retrofitting efforts. RVS is a simple yet effective method, [11]. The methodology employed in the RVS procedure relies on conducting a walkway inspection of a structure and completing a Data Collection Survey Form by the surveyor after visually examining the structure externally and, when possible, internally, without engaging in complex computations, [12]. The first step was research planning, which involved pre-field planning activities, pre-field data collection, and preliminary site investigation. The pre-field planning activities include selecting the data collection forms, training the screeners to conduct the RVS, and the review of the acquired data. The next step is the execution of rapid visual screening. The final section involves analyzing the collected data, [13]. Using the FEMA P-154 RVS checklist, the researchers determine each building's vulnerability score. Buildings with a score of two or below are advised to undergo a more thorough evaluation, [14]. While Rapid Visual Screening (RVS) may lack the precision of detailed modeling, it provides a simple and effective approach for identifying parts of a city prone to earthquake vulnerability, [15], [16], [17].

2.3.2 Phase 2: Structural Modelling of PSU Buildings

Acquire architectural and structural plans from the university's physical plant office and verify dimensions through on-site measurements. A rebound hammer test will be used to estimate the compressive strength of the concrete materials used in the structures. This involves selecting representative samples of critical exterior columns and beams, with three test locations chosen for each beam and column. The Schmidt hammer, commonly known as a Swiss hammer or rebound hammer, is a specialized tool to evaluate the rebound or elasticity of materials like concrete and rock, [18]. Its primary function lies in determining surface hardness and resistance to penetration. Acquire exposed rebars at the top of columns and conduct a tensile test using a Universal Testing Machine (UTM) to assess the tensile strength of reinforcing bars. The following are the procedures for creating a three-dimensional frame model of the structure in SAP 2000, [19].

1. Specify the grid system and develop a three-dimensional frame model of the structure, including the dimensions, shapes, and arrangements of various structural elements.
2. Define material and geometric properties for each structural element, such as material properties of concrete and rebars, section properties, and boundary conditions.
3. Define the load pattern and assign a gravity load.

2.3.3 Phase 3: The Capacity Spectrum Method

The Capacity Spectrum Method (CSM), a performance-based seismic evaluation approach, determines a structure's seismic capacity, [20]. This process involves generating the structure's capacity curve by performing a pushover analysis. Response spectra illustrate the demands of the seismic ground motion, [21]. The intersection of the capacity and demand curves is known as the performance point. The capacity curve was derived using pushover curves employing traditional pushover analysis, and the demand curve was derived from the inelastic response spectra of specific ground motion recordings, [22]. The Capacity Spectrum Method (CSM) was conducted using the following methodologies:

1. Perform pushover analysis on the PSU building structural model using SAP 2000.
2. Acquire ground motion data from the Incorporated Research Institutions for Seismology (IRIS). Find the normalized Peak Ground Acceleration (PGA). The normalized ground motion data is produced by scaling the original ground motion data up and down, [23]. Convert normalized PGA into a response spectrum through SeismoSignal.

$$\text{PGA}_{\text{Normalized}} = (\text{GMD}) \left(\frac{\text{PGA}_{\text{Excitation}}}{\text{PGA}_{\text{Maximum}}} \right) \tag{1}$$

where:
GMD = Ground Motion Data
$\text{PGA}_{\text{Excitation}}$= the level of excitation ranges from peak ground acceleration (PGA) values, starting from 0.1 g up to 3.0 g.
$\text{PGA}_{\text{Maximum}}$=absolute maximum ground motion data

3. Determine the performance points by analyzing the intersection of the capacity and response spectrum curves. Several values of performance points are obtained by scaling the demand curve into various excitation levels, ranging from 0.1 g to 3.0 g.

2.3.4 Phase 4: Development of Seismic Fragility Curves.

Fragility curves show the risk of structural damage caused by varying levels of ground shaking. An analytical method was used to produce these fragility curves, and the following is a thorough step-by-step procedure, [24], [25].

1. Determine the damage state threshold using Table 4 and the data (yield displacement and ultimate displacement) from the pushover curve to calculate the limits of spectral displacement for each damage state.
2. Establish the damage ranking by applying the calculated damage state thresholds.
3. Determine the damage states corresponding to all displacement performance points obtained from the capacity curve and response spectrum.

Table 4. Damage State Threshold Values, [26],[27]

Damage State	Damage Rank	Spectral Displacement
No Damage	D	0
Slight	C	0.7dy
Moderate	B	dy
Extensive	A	$[\text{dv} + 0.25(\text{du} - \text{dv})]$
Complete	As	Du

Where:
dy = yield displacement, **du** = ultimate displacement

4. Count the frequency of occurrence for each damage state threshold with the performance points.
5. Compute the damage ratio by obtaining the total cumulative probability of occurrence. This ratio is calculated by dividing the number of occurrences by the total number of records at a specific Peak Ground Acceleration (PGA) level.

6. Determine the standard deviation and mean accordingly. The mean and standard deviation were obtained for every damage state using equations (2) and (3). The lognormal values of PGAs were then multiplied by each frequency to provide lognormal values for the standard deviation and mean.

$$\lambda = \frac{\sum x}{N} \tag{2}$$

$$\xi = \sqrt{\frac{\sum (x-\lambda)^2}{N-1}} \tag{3}$$

Where:
x = individual ground motion data obtained
N= sample size of ground motion data
λ = mean of the ground motion data
ξ = standard deviation

7. The probability of exceedance (Pr) may be calculated by applying equation (4).

$$\boldsymbol{Pr} = \Phi \left[\frac{\{ln(X) - \lambda\}}{\xi}\right] \tag{4}$$

Where:
Pr=probability of exceedance
x = peak ground acceleration
λ = mean
ξ = standard deviation
Φ =standard normal deviation

8. Plot the likelihood of exceedance versus the peak ground acceleration (PGA) excitation level to create seismic fragility curves for the PSU buildings.

3 Results and Discussion

3.1 Rapid Visual Screening (RVS) Results

The RVS scores of all 11 school buildings are displayed in Figure 5. Three of the buildings have scores below 2.0, which is the FEMA P-154 cutoff score. Eight of the eleven school buildings had ratings higher than 2, indicating better seismic performance. Engineering Buildings 1 (BLDG4), Engineering Buildings 2 (BLDG5), and Engineering Buildings 3 (BLDG6) had scores lower than the cutoff of 2. This suggests that a more thorough examination of these structures is required to precisely determine their vulnerability to seismic risks.

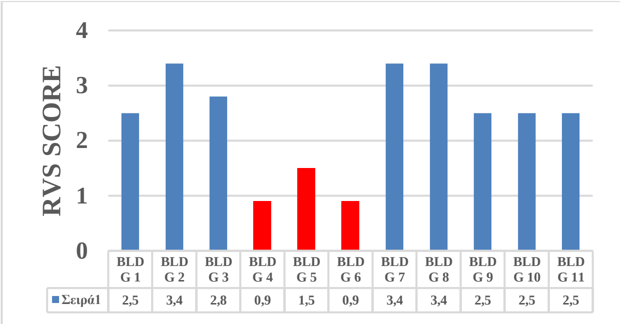

Fig. 5: RVS Score

3.2 Structural Modelling of PSU Buildings

Out of the eleven school buildings, Engineering Buildings 1 (BLDG4), Engineering Buildings 2 (BLDG5), and Engineering Building 3 (BLDG6) had scores that were below the cutoff of 2, indicating the need for a more thorough investigation using fragility analysis. The structural model was created based on architectural and structural plans, and material properties were incorporated using SAP 2000. All the buildings' main structural elements are included in the structural modeling, with the focus of the research being on the beams, girders, and columns that make up the structure. Accordingly, the finished structural models of school buildings are shown in isometric perspective in Figure 6, Figure 7 and Figure 8.

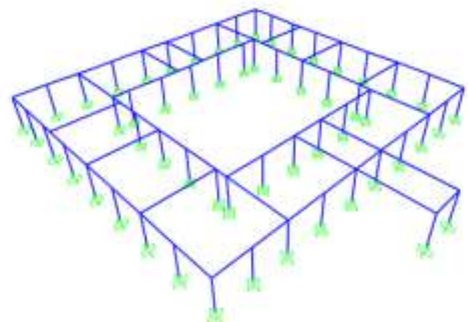

Fig. 6: Structural Model of Engineering Building 1

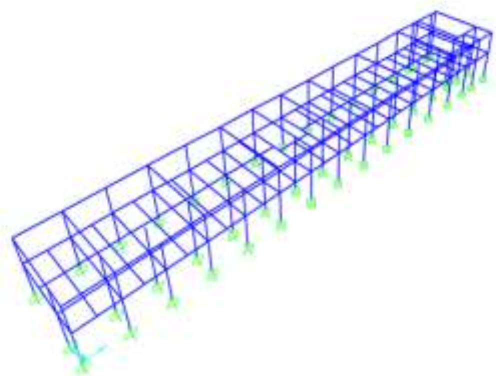

Fig. 7: Structural Model of Engineering Building 2

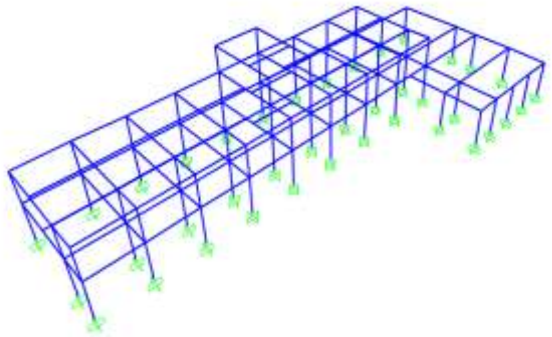

Fig. 8: Structural Model of Engineering Building 3

3.2.1 Rebound Hammer Test

The rebound hammer test was conducted on the school buildings to estimate the on-site compressive strength of the concrete structures. The procedure involves pressing the device against the concrete surface until the hammer impacts the surface a designated number of times at each test location. The resulting readings from these impacts are interpreted using a rebound hammer test chart, and the average of these readings is used to determine the compressive strength. A thorough explanation of the methodologies for performing a rebound hammer test is available in the American Standards for Testing and Materials (ASTM C805) journal, [28]. Tests were carried out for one column and beam in each building at three locations close to supports and at midspan. Instead of conducting tests on each column and beam, a sampling strategy was implemented. This method focused on selecting a representative sample of each building's critical exterior columns and beams. Specifically, three test locations were carefully chosen for each beam and column. Ten readings should be taken from each test area and averaged to determine the compressive strength. Table 5 (Appendix) summarizes the compressive strength used for each building obtained from the rebound hammer test.

3.2.2 Tensile Test

The exposed rebars at the top of columns were obtained for each building to assess the tensile strength of reinforcing bars. The sample steel bars were tested using the Universal Testing Machine at the authorized materials testing and geotechnical engineering laboratory facility. During the tensile test, the material specimen is subjected to a gradually increasing axial load until it reaches the point of failure or fracture, as shown in Figure 9. The yield point and ultimate tensile strength summary were determined as shown in Table 6 (Appendix) and used in the structural model as material properties.

Fig. 9: Fractured Specimen of Engineering Building 1

3.3 The Capacity Spectrum Method as a Structural Assessment Methodology

3.3.1 Pushover Curve

Figure 10, Figure 11 and Figure 12 display the pushover curves for Engineering Building 2, Engineering Building 1, and Engineering Building 3 along X- and Y-directions. The graphs depict the relationship between displacement (x-axis) and base shear force (y-axis). The peak point on the pushover curve indicates the structural material's capacity to withstand maximum lateral loads. In contrast, the yield point indicates the structure’s boundary within the elastic range, [29]. By utilizing the yielded displacement (dy) and ultimate displacement (du) and inputting these values into the equations outlined in Table 2 (Appendix), one can calculate the damage thresholds for each damage state accordingly. In Engineering Building 2, as depicted in Figure 10, the yield point was reached in the x-direction at a base shear force of 3026.783 kN, corresponding to a displacement of 20.079 mm. The maximum displacement, on the other hand, was recorded at 173.476 mm, with the structure enduring a base shear force of 3402.297 kN. Similarly, in the y-direction, the yield point was observed at a base shear force of 1796.186 kN with a displacement of 26.437 mm, while the maximum displacement of 263.273 mm occurred at a base shear force of 2089.338 kN. The maximum base shear force of 3402.297 kN in the x-direction is higher than 2089.338 kN in the y-direction. This result suggests that Engineering Building 2 can sustain a greater base shear force in the x-direction, indicating that this is the building's strongest axis. In contrast, Engineering Buildings 1 and 3 can tolerate higher base shear force in the y-direction, as shown in Figure 11 and Figure 12, respectively, implying that the y-direction is the strongest axis for these buildings.

DOI: 10.37394/232015.2024.20.75

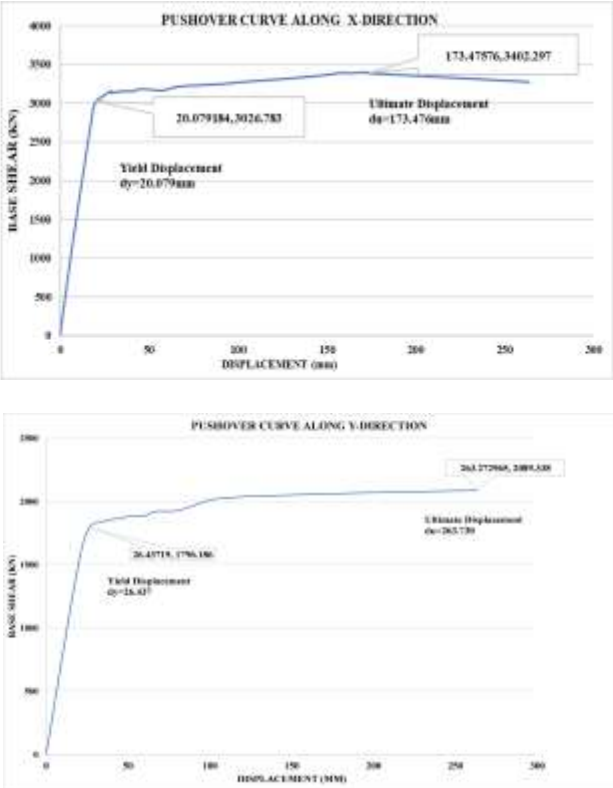

Fig. 10: Pushover Curve of Engineering Building 2 in the X and Y directions

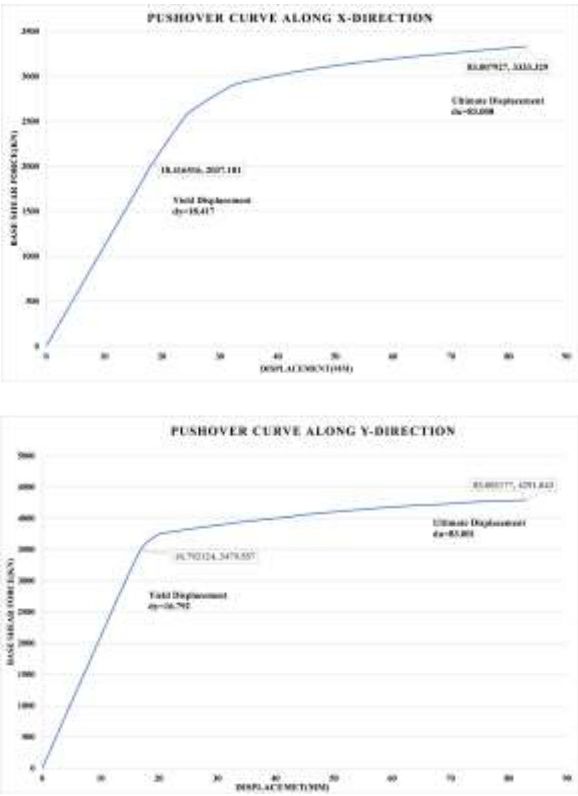

Fig. 11: Pushover Curve of Engineering Building 1 in the X and Y-direction

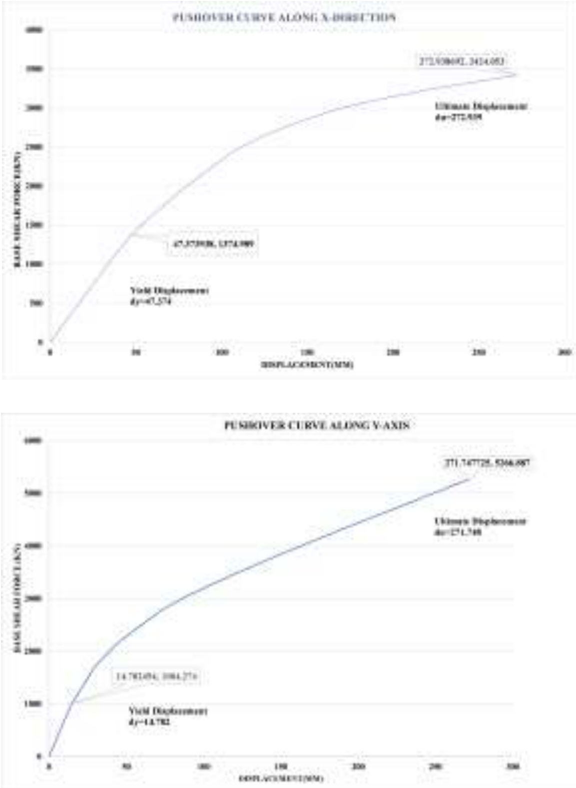

Fig. 12: Pushover Curve of Engineering Building 3 long X and Y-direction

3.3.2 Ground Motion Inputs

All ground motion records are obtained from the Incorporated Research Institutions for Seismology (IRIS), as shown in Figure 13. For these records, 12 actual local and foreign earthquake events are considered, as shown in Appendix in Table 1 and Table 2. Using Microsoft Excel, each ground motion has been normalized and scaled accordingly from 0.1g to 3.0g, as shown in Figure 14. There are 720 scaled earthquake recordings when the elastic response spectra of the East-West and North-South directions are considered for each event. As seen in Figure 15, the response spectra are obtained using SeismoSignal software. The response spectra were run in SAP 2000 and converted to demand spectrum.

Fig. 13: Ground Motion Records from Incorporated Research Institutions for Seismology (IRIS)

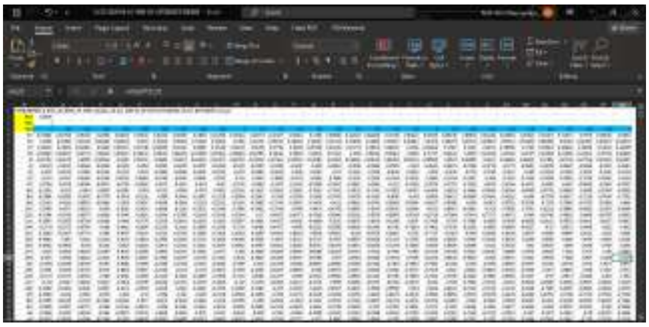

Fig. 14: Normalized Peak Ground Acceleration of Luzon Earthquake (02-24-1988) of magnitude of 7.2

Fig. 15: Response Spectra based on Luzon Earthquake (02-24-1988) of magnitude 7.2 with 0.1g PGA along East-West direction using SeismoSignal Software

3.3.3 Capacity Spectrum Method (CSM)

The capacity spectrum approach defines the performance point as the intersection of the capacity and response spectrum curves. Following the ATC-40 Capacity Spectrum Method (CSM), the capacity curve obtained from the pushover curve can be superimposed onto the demand spectrum curve, [30]. Several performance point values are obtained by scaling the demand curve into various excitation levels between 0.1 g and 3.0 g. A total of 1440 performance points were determined for a single model in the east-west and north-south directions, corresponding to 12 ground motion records.

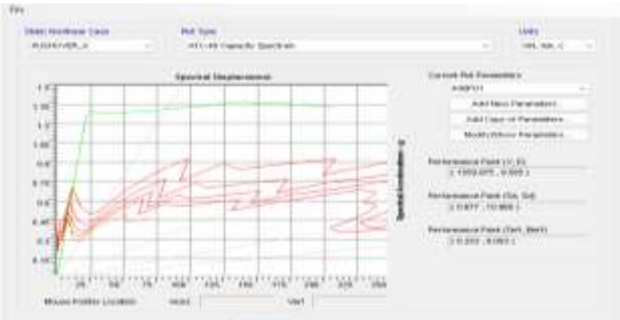

Fig. 16: Capacity Curve based on July 16, 1990 Luzon, Philippine's earthquake with 1.0g PGA based on magnitude 6.5 in the east-west direction at X-axis of Engineering Building 2

Figure 16 illustrates the superimposed capacity curve sample for Engineering Building 2 at 1.0 g PGA, corresponding to a magnitude 6.5 earthquake in Luzon, Philippines, on July 16, 1990. A summary of performance points achieved when the Engineering Buildings 2 model in SAP 2000 was exposed to an earthquake of magnitude 6.5 that occurred on July 16, 1990, in Luzon, Philippines, is shown in Table 7 (Appendix).

3.4 Development of Seismic Fragility Curves

3.4.1 Damage State Threshold Limits

The spectral displacement for the buildings on both x and y axes is determined in this study by applying the approach, shown in Table 4. The data presented in Table 8 (Appendix) outline the structural damage state thresholds for both the y-axis and x-axis directions of each school building. In addition to the no-damage condition (D), the damage thresholds used in this study are categorized into four groups: slight damage (C), moderate damage (B), extensive damage (A), and complete damage (As).

Table 8 (Appendix) shows that the spectral displacement values for C and B are small in both the x and y directions. Damage thresholds with small values have a higher likelihood of being exceeded. The damage thresholds for A and As are comparatively greater than the spectral displacements for C and B. For example, Engineering Building 2 displayed a damage threshold of 173.476 mm for As in the x-direction. This indicates that to achieve "complete damage," a spectral displacement of 173.476mm is required. This data was then used to determine the damage rank and generate a set of fragility curves.

3.4.2 Damage Ranking

The provided tabulated data for the damage ranking was generated utilizing the acquired performance points and the damage state threshold limits. Table 9 (Appendix) depicts the performance points associated with scaled peak ground acceleration values and the corresponding damage rankings for Engineering Building 2 along the East-West direction (x-axis), derived from data recorded during the magnitude 8.0 earthquake near the east coast of Peru on August 15, 2007. The data indicates higher damage states correspond to higher peak ground acceleration values. Specifically, Table 9 (Appendix) shows that Engineering Building 2 sustained complete damage (As) at a peak ground acceleration of 2.0 g during this seismic event.

3.4.3 Probability of Occurrence

The Occurrences of earthquakes for each damage state threshold were tallied using the performance points. Table 10 (Appendix) summarizes the occurrence frequency for different damage conditions observed in Engineering Building 2 along the y-axis in the East-West direction based on varying levels of peak ground acceleration (PGA) measured in gravitational units (g). This table generates a graph showing the probability of occurrence for each damage situation. The cumulative damage ratios, representing the correlation between each damage rank and its corresponding PGA value, were the basis for constructing the probability of occurrence graphs. Figure 17, Figure 18 and Figure 19 illustrate the percentage of each damage rank associated with the PGA. These graphs indicate that the damage rank consistently rises as the PGA increases from 0.1 g to 3.0 g.

For Engineering Building 2, as shown in Figure 17, the graph illustrates the probability of occurrence of different damage conditions for Engineering Building 2 along the y-direction as a function of peak ground acceleration (PGA). At PGA's up to 0.4 g, the probability of experiencing no damage to slight damage (state D) is 100%, indicating that the building remains mostly intact. As the PGA increases from 0.5 g to 1.2 g, the building will experience slight to moderate damage (states C and B). This range indicates that the building suffers from minor structural issues that gradually escalate as the seismic intensity increases.

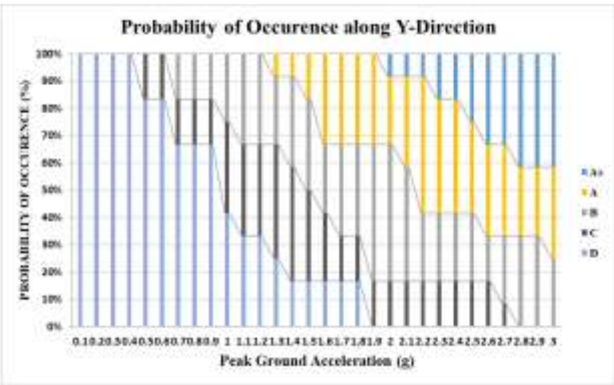

Fig. 17: Probability of Occurrence for Engineering Building 2 in the East-West Direction(y-axis).

The building sustains moderate to extensive damage as we approach 1.3 g-1.9 g (states B and A). This suggests that at these levels of seismic activity, the building's structural integrity is compromised to a greater extent, resulting in substantial damage that may require significant repairs or lead to partial structural failure. Finally, the structure will experience extensive to complete damage in the 2.0 g–3.0 g range (states A and As). This indicates that the building will likely to experience catastrophic structural failure, leading to complete damage.

Figure 18 illustrates the probability that Engineering Building 1 will receive slight to moderate damage, ranging from 0.5 g to 1.3 g, along the east-west direction along the y-axis. The building sustains moderate to extensive damage as we get closer to 1.4 -2.8g. Finally, the structure will undergo extensive damage, ultimately leading to complete damage within the 2.9–3.0g range.

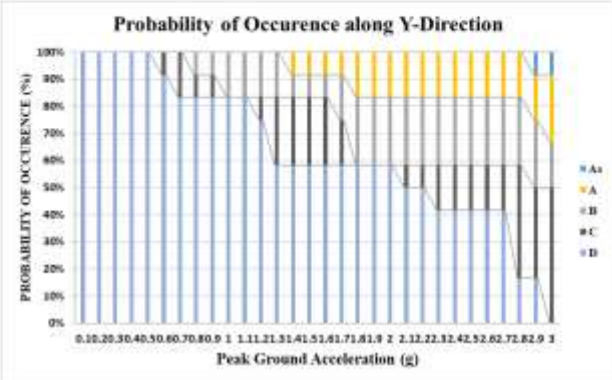

Fig. 18: Probability of Occurrence for Engineering Building 1 in East-West Direction (Y-axis)

Figure 19 depicts the likelihood of Engineering Building 3 experiencing slight to moderate damage between 0.2 g and 1.1 g in the east-west direction (y-axis). The building sustains moderate to extensive damage as we approach 1.2-2.6 g. Finally, the structure will experience extensive to complete damage in the 2.7–3.0 g range.

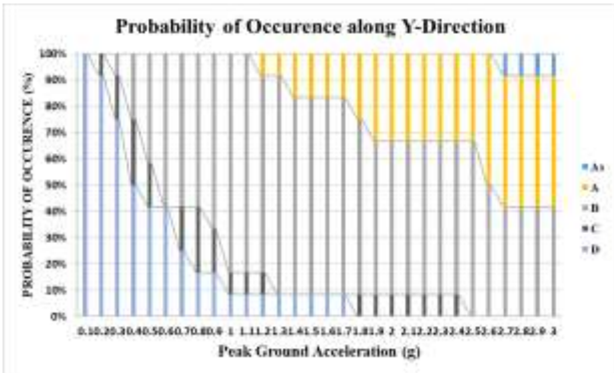

Fig. 19: Probability of Occurrence for Engineering Building 3 in East-West Direction (y-axis)

3.4.4 Fragility Curves

The fragility curves evaluate the likelihood of reaching or exceeding each damage condition (slight, moderate, extensive, and complete) over peak ground accelerations (PGA) from 0.1 g to 3.0

DOI: 10.37394/232015.2024.20.75

g. The probabilities (Pr) for each damage condition were shown on a single graph, resulting in a clear and interpretable representation in Appendix in Figure 20, Figure 21 and Figure 22.

In practical terms, the "D" or "No Damage" condition should be excluded from the fragility curves, [29]. The figures show the probabilities for exceeding a damage condition with its associated scaled peak ground acceleration.

For Engineering Building 2, depicted in Figure 20 (Appendix), the likelihood of surpassing the specified ground acceleration of 0.4 g is as follows: in the east-west direction along the X-axis, it's 23.41%, 5.49%, 5.20%, 5.22%, and 5.47% for no damage (D), slight damage (C), moderate damage (B), extensive damage (A), and complete damage (As), respectively. Along the Y-axis, it's 43.30%, 7.50%, 5.61%, 5.20%, and 5.29% for the same corresponding levels of damage. Likewise, in the north-south direction along both the X and Y axes, the probabilities of surpassing a peak ground acceleration of 0.4 g are as follows: 17.52%, 5.55%, 5.19%, 5.21%, and 5.39% for no damage (D), slight damage (C), moderate damage (B), extensive damage (A), and complete damage (As), respectively. Along the Y-axis, the probabilities are 40.09%, 6.26%, 5.34%, 5.19%, and 5.27% for the same levels of damage.

As illustrated in Figure 21 (Appendix), the probabilities of exceeding a peak ground acceleration of 0.4 g for Engineering Building 1 in the east-west direction along the X and Y axes are 40.17%, 6.53%, 5.46%, 5.25%, and 5.23%, and 18.89%, 5.35%, 5.32%, 5.19%, and 5.44%, respectively. These probabilities correspond to damage levels of no damage (D), slight damage (C), moderate damage (B), extensive damage (A), and complete damage (As). Similarly, in the north-south direction along the X-axis, the probabilities of exceeding a peak ground acceleration of 0.4g are 39.98% for no damage (D), 6.74% for slight damage (C), 5.38% for moderate damage (B), 5.19% for extensive damage (A), and 5.33% for complete damage (As). Along the Y-axis, the probabilities are 18.15% for no damage (D), 5.31% for slight damage (C), 5.25% for moderate damage (B), 5.23% for extensive damage (A), and 0% for complete damage (As).

As illustrated in Figure 22 (Appendix), the probabilities of exceeding a peak ground acceleration of 0.4 g for Engineering Building 3 in the east-west direction along the X-axis are 55.46%, 21.98%, 8.07%, 5.31%, and 5.24%. Along the Y-axis, the probabilities are 53.88%, 21.07%, 6.84%, 5.19%, and 5.39%. These values correspond to damage levels of no damage (D), slight damage (C), moderate damage (B), extensive damage (A), and complete damage (As), respectively. Similarly, in the north-south direction along the X-axis, the probabilities of exceeding a peak ground acceleration of 0.4 g for Engineering Building 3 are 53.96% for no damage (D), 18.18% for slight damage (C), 6.24% for moderate damage (B), 5.22% for extensive damage (A), and 5.24% for complete damage (As). Along the Y-axis, the probabilities are 54.23% for no damage (D), 17.62% for slight damage (C), 6.82% for moderate damage (B), 5.19% for extensive damage (A), and 5.33% for complete damage (As). The resulting fragility curves indicate that as peak ground acceleration increases, the likelihood of exceeding all damage states also rises.

The study considered the seismic requirements outlined in the National Structural Code of the Philippines (NSCP), focusing on the probability of exceedance (Pr) for the "complete damage (As)" state. This assessment involved evaluating the impact of a 0.4 g PGA earthquake along the east-west and north-south axes of each building. According to the NSCP, structures in the Philippines are designed to endure a peak ground acceleration of 0.4g with a 10% probability of exceedance,[31], which is also included in the CSIRO handbook entitled "Designing Resilient", [32]. An extract from the book mentioned above is presented in Figure 23.

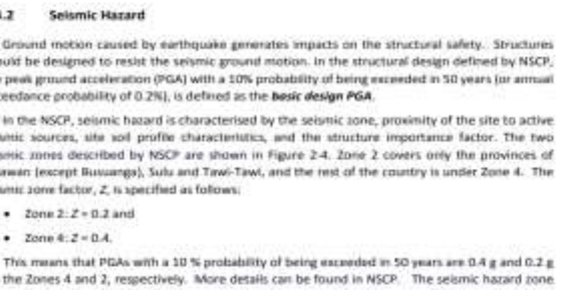

2.3.2 Seismic Hazard

Ground motion caused by earthquake generates impacts on the structural safety. Structures should be designed to resist the seismic ground motion. In the structural design defined by NSCP, the peak ground acceleration (PGA) with a 10% probability of being exceeded in 50 years (or annual exceedance probability of 0.2%), is defined as the ***basic design PGA***.

In the NSCP, seismic hazard is characterised by the seismic zone, proximity of the site to active seismic sources, site soil profile characteristics, and the structure importance factor. The two seismic zones described by NSCP are shown in Figure 2-4. Zone 2 covers only the provinces of Palawan (except Busuanga), Sulu and Tawi-Tawi, and the rest of the country is under Zone 4. The seismic zone factor, Z, is specified as follows:

- Zone 2: Z = 0.2 and
- Zone 4: Z = 0.4.

This means that PGAs with a 10 % probability of being exceeded in 50 years are 0.4 g and 0.2 g for the Zones 4 and 2, respectively. More details can be found in NSCP. The seismic hazard zone related to each local government is listed in Appendix A.

Fig. 23**:** Basic Design PGA

In addition to the NSCP provision, the Structural Engineers Association of California (SEAOC) has the following excerpt: "A structure with 30 or more-year lifespan is not SAFE when subjected to a seismic event with a 10% probability of exceeding the collapse or complete damage. The structure, being more than 50 years old, is vulnerable to large-magnitude earthquakes", [33].

Table 11.A (Appendix) shows that under the condition of complete damage (As), the probabilities of exceedance for Engineering Buildings 1, 2, and 3 in the East-West direction

remain relatively consistent, with maximum values of approximately 5%. Similarly, as summarized in Table 11.B (Appendix), the probabilities of exceedance at 0.4g PGA for complete damage (As) in the North-South direction are approximately 5% for Engineering Buildings 2 and 3. However, Engineering Building 1 demonstrates a 0% probability of exceedance under the complete damage (As) condition in the Y-Axis, indicating no vulnerability to this level of seismic loading for this building. Furthermore, fragility curve analysis, which evaluates the likelihood of structural damage under seismic events, revealed that none of these three buildings exceeded the 10% probability of exceedance at 0.4 g PGA under "complete damage (As)." This analysis conforms to the criteria established by the National Structural Code of the Philippines (NSCP) for buildings in Seismic Zone 4, demonstrating that the structures are safe for occupancy and do not require retrofitting measures.

The maximum peak ground acceleration (PGA) values that Engineering Building 1 can withstand with a 10% likelihood of exceedance are displayed by the generated fragility curves shown in Table 12.A and Table 12.B in Appendix. In the east-west direction(x-axis), the building can endure slight damage of up to 0.50 g, moderate damage of up to 0.53 g, extensive damage of up to 0.55 g, and collapse damage of up to 0.60 g. Along the y-axis in the same direction, the building can withstand slight damage of up to 0.55 g, moderate damage of up to 0.56 g, extensive damage of up to 0.59g, and collapse damage of up to 0.60g. Similarly, in the north-south direction along the x-axis, the analysis revealed that Engineering Building 1 could withstand the following maximum peak ground accelerations (PGA) for potential earthquakes: 0.49 g for 'slight damage', 0.54 g for 'moderate damage', 0.58 g for 'extensive damage', and 0.60 g for 'collapse damage. Along the y-axis in the north-south direction, the building can withstand slight damage of up to 0.56g, moderate damage of up to 0.57g, and extensive damage of up to 0.58g.

The analysis of Engineering Building 2 indicates its ability to withstand various levels of peak ground acceleration (PGA) with a 10% probability of exceedance. Along the east-west direction (x-axis), the building can sustain slight damage of up to 0.55 g, moderate damage of up to 0.58 g, extensive damage of up to 0.58 g, and collapse damage of up to 0.60g. Along the y-axis in the same direction, it can endure slight damage of up to 0.46 g, moderate damage of up to 0.53 g, extensive damage of up to 0.57 g, and collapse damage of up to 0.60g.In the north-south direction (x-axis), Engineering Building 2 can withstand slight damage of up to 0.55 g, moderate damage of up to 0.59 g, extensive damage of up to 0.60 g, and collapse damage of up to 0.60 g. Along the y-axis in this direction, it can sustain slight damage of up to 0.50 g, moderate damage of up to 0.56 g, extensive damage of up to 0.59 g, and collapse damage of up to 0.60 g.

The seismic fragility curves for Engineering Building 3 in the east-west orientation show its ability to withstand various levels of peak ground acceleration (PGA) with a 10% probability of exceedance. Along the x-axis, the building can endure slight damage of up to 0.25 g, moderate damage of up to 0.43 g, extensive damage of up to 0.56 g, and collapse damage of up to 0.60 g. Along the y-axis in the same orientation, it can sustain slight damage of up to 0.25 g, moderate damage of up to 0.48 g, extensive damage of up to 0.58 g, and collapse damage of up to 0.60 g. In the north-south (x-axis), Engineering Building 3 can withstand slight damage of up to 0.29 g, moderate damage of up to 0.50 g, extensive damage of up to 0.58 g, and collapse damage of up to 0.58 g. Along the y-axis in this direction, it can endure slight damage of up to 0.29 g, moderate damage of up to 0.48g, extensive damage of up to 0.58 g, and collapse damage of up to 0.60g.

The maximum peak ground acceleration (PGA) associated with a 10% probability of exceedance for every damage condition for all structures is displayed in Appendix in Table 12.A and Table 12.B. The results indicate that all three buildings would sustain "complete damage (As)" at a maximum PGA of 0.60 g. Consequently, it was determined that these buildings can withstand a maximum of 0.60 g, which exceeds the Philippine National Structural Code's (NSCP) minimum standard of 0.4g. According to the Modified Mercalli Scale, a PGA of 0.60 g corresponds to Intensity VIII, characterized as "severe" shaking, [34]. This level of shaking can cause significant structural damage and pose serious risks to occupants and safety. If seismic activity exceeds a PGA of 0.60 g, the structures will likely sustain irreparable damage, rendering them unsafe for occupancy. Additionally, the findings are in Appendix in Table 12.A and Table 12.B align with the pushover curve results shown in Figure 10, Figure 11 and Figure 12, validating the directional strengths of the buildings and confirming the accuracy of the pushover analysis. When a structure can withstand a higher PGA in the x-direction than the y-direction, it signifies that the structural integrity, reinforcements, and design along the x-axis are more robust. This is often observed through higher base shear forces and greater peak ground accelerations in that direction during analysis, [35]. Specifically, for Engineering Building 2, the base shear force in the x-direction is 3402.297 kN, significantly higher than the 2089.338 kN in the y-direction, as shown in Figure 10. This disparity indicates that Engineering Building 2 can withstand a greater base shear force in the x-direction, identifying it as the building's strongest axis. This conclusion is further supported by consistently higher peak ground acceleration values for all damage states in the x-direction compared to the y-axis, as shown in Appendix in Table 12.A and Table 12.B. Similarly, for Engineering Buildings 1 and 3, the results show larger peak ground accelerations in the y-direction than in the x-direction, demonstrating that the y-direction is the strong axis, confirming the results obtained from the pushover curve as shown in Figure 11 and Figure 12.

4 Conclusion

Three buildings, namely Engineering Buildings 1 (BLDG4), Engineering Buildings 2 (BLDG5), and Engineering Buildings 3 (BLDG6), with seismic scores below the RVS FEMA P-154 cutoff of 2.0 underscore the importance of conducting further detailed assessments that go beyond simple RVS scores. These comprehensive evaluations are crucial for precisely determining the level of vulnerability of these buildings to seismic risks using fragility analysis. By integrating comprehensive evaluation data, such as detailed structural modeling, site-specific ground motion characteristics, and historical earthquake data, the fragility analysis becomes more robust. This allows for a more precise determination of the seismic performance of the buildings, leading to more accurate predictions of potential damage.

Furthermore, the analysis of the fragility curves showed that Engineering Building 1, Engineering Building 2, and Engineering Building 3, under the condition of "complete damage (As)," demonstrated a maximum probability of exceedance (Pr) of 5% at 0.40 g PGA. Because no value was more than 10%, this result fulfills the minimum requirement set by the National Structural Code of the Philippines (NSCP) for structures in Seismic Zone 4. Consequently, these buildings are declared safe for occupancy and do not require retrofitting measures.

Moreover, the fragility curve analysis indicates that Engineering Building 1, and Engineering Building 2 have a low probability, below 10%, of experiencing any damage from slight to complete during seismic events. However, Engineering Building 3 shows a higher likelihood of sustaining slight damage, with a lower probability of experiencing moderate to complete damage. This suggests that while Engineering Building 3 may suffer minor damage like hairline cracks and non-structural component failures, it remains safe for occupancy during most seismic events.

Finally, the results showed that Engineering Building 1, Engineering Building 2, and Engineering Building 3 would sustain "complete damage (As)" at a maximum PGA of 0.60 g PGA. Consequently, it was discovered that these buildings can tolerate a maximum of 0.60 g, surpassing the minimum standard of 0.4 g set by the National Structural Code of the Philippines . According to the Modified Mercalli Scale, a peak ground acceleration (PGA) of 0.60g corresponds to Intensity VIII, described as "severe" shaking, [36]. As peak ground acceleration (PGA) increases, the probability of exceeding each damage rank concurrently rises, as shown in the resulting fragility curves. The fragility curve indicates that the structure becomes highly vulnerable during high PGA events. In the event of an earthquake with a recorded PGA exceeding 0.60g, the structure has a high probability of collapsing. Additionally, the analysis reveals that Engineering Building 2 experienced higher peak ground acceleration (PGA) along its y-axis. This can be attributed to the y-axis being structurally stronger, as confirmed by the results from the pushover analysis. Therefore, the structural components along the x-axis of Engineering Building 2 were deemed more significant. Similarly, Engineering Buildings 1 and 3 show larger peak ground accelerations in the y-direction than in the x-direction, demonstrating that the y-direction is the strong axis.

Acknowledgement:
The authors would like to thank Pangasinan State University (PSU) Urdaneta Campus for permitting them to conduct the study.

Declaration of Generative AI and AI-assisted Technologies in the Writing Process

During the preparation of this work the authors used QuillBot in order to improve the readability and language of the manuscript. After using this tool, the authors reviewed and edited the content as needed and take full responsibility for the content of the publication.

References:

[1] D. Paton, E. Anderson, J. Becker, and J. Petersen, "Developing a comprehensive model of hazard preparedness: lessons from the Christchurch earthquake," *International Journal of Disaster Risk Reduction*, vol. 14, no. 1, pp. 37-45, 2015. doi: 10.1016/j.ijdrr.2014.11.011.

[2] C. Baclig, "Dying in an earthquake: Experts say it's not just the tremor," Inquirer.Net, July 28, 2022, [Online]. https://newsinfo.inquirer.net/1636640/dying-in-an-earthquake-experts-say-its-not-just-the-tremor (Accessed Date: July 27, 2024).

[3] M. Medina, "Devastating 'faults' of the 'Big One,'" *Inquirer Business*, Apr. 27, 2019, [Online]. https://business.inquirer.net/269314/devastating-faults-of-the-big-one/amp (Accessed Date: July 27, 2024).

[4] A. W. Oreta, R. De Jesus, M. E. Grio, R. Mendoza Jr., L. Garciano, R. Ibabao, G. Sevieri, and C. Galasso, "Seismic screening and structural investigation of heritage buildings for adaptive reuse: a survey study at Iloilo City, Philippines," *The 9th AUN/SEED-Net Regional Conference on Natural Disaster (RCND 2021), IOP Conf. Series: Earth and Environmental Science*, Canada, 2022, pp.1-10. doi: 10.1088/1755-1315/1091/1/012008.

[5] R.V. Garrote, R.C. Ilumin, "Comparative Analysis on Seismic Provisions of the National Structural Codes of the Philippines (NSCP) 1992 and 2010 as applied to the Design of Reinforced Concrete Public School Building," *Proc. Of Sixth International Conference on Advanced in Civil Structural and Mechanical Engineering*, Thailand, 2017, pp. 62-67, [Online]. https://ewr1.vultrobjects.com/ired/papers/3522/2ee800e32c0981d9f9919a05db3534ea.pdf (Accessed Date: July 27, 2024).

[6] R.C. Ilumin, A.W. Oreta, "A Post-Disaster Functional Asset Value Index for school buildings," *Procedia Engineering*, Bangkok, Thailand, Jan. 2018, pp. 230–237. doi: 10.1016/j.proeng.2018.01.030.

[7] M. A. Llego, "2019 DePED guidelines on schools used as evacuation center," *TeacherPH*, Mar. 15, 2019, [Online]. https://www.teacherph.com/guidelines-schools-evacuation-center/ (Accessed Date: July 27, 2024).

[8] R. Gentile, C. Galasso, Y. Idris, I. Rusydy, E. Meilianda, "From rapid visual survey to multi-hazard risk prioritisation and numerical fragility of school buildings," *Natural Hazards and Earth System Sciences*, vol. 19, no. 7, pp. 1365–1386, Jul. 2019. doi: 10.5194/nhess-19-1365-2019.

[9] R. De Guzman, "DOST'S Fault Finder", *Department of Science and Technology*, Oct. 05, 2024, [Online] https://www.dost.gov.ph/knowledge-resources/news/48-2017-news/1223-dost-s-fault-finder.html (Accessed Date: July 27,2024)

[10] M.B. Baylon, "Seismic vulnerability assessment of Adamson University buildings As-built using fragility curves," *Global Journal of Research in Engineering*, vol.18, no.1, pp. 29-49, 2018, [Online] https://engineeringresearch.org/index.php/GJRE/article/view/1785 (Accessed Date: July 27, 2024)

[11] S. U. Khan, M.I. Qureshi, I. A. Rana, A. Maqsoom, "Seismic vulnerability assessment of building stock of Malakand (Pakistan) using FEMA P-154 method*," SN Applied Sciences/SN Applied Sciences*, vol. 1, no. 12, pp. 1-14, Nov. 2019. doi: 10.1007/s42452-019-1681-z.

[12] J. Dapito, D. Barrozo, R. Panis, A. Cañete, R. Orbeso, K. Yagi, R. Salazar, "Two-Dimensional Analysis Vulnerability Assessment of Public Secondary Buildings in District II of Manila,"*8th IEEE International Conference Humanoid, Nanotechnology, Information Technology Communication and Control, Environment and Management (HNICEM)*, Cebu, Philippines, Dec. 2017, pp.1-7. doi: 10.1109/HNICEM.2015.7393217

[13] I.V.P. Perez, L.J. David, S.P. Rodrigo, C.J. Sibug, G.H. Arcilla, C.B. Nava, L. Manuntag, C.J. Coronel, "Assessment of the seismic vulnerability of San Guillermo parish church and San Agustin parish church in Pampanga," *International Journal of Advance Research, Ideas and Innovations in Technology*, vol. 9, no. 2, pp. 487-515, June 2023, [Online] https://www.ijariit.com/manuscripts/v9i2/V9I2-1340.pdf (Accessed Date: July 27, 2024)

[14] S. A. El-Betar, "Seismic vulnerability evaluation of existing R.C. buildings*," HBRC Journal/HBRC Journal*, vol. 14, no. 2, pp. 189–197, Aug. 2018. doi: 10.1016/j.hbrcj.2016.09.002.

[15] S.F. Shah, A. Ahmed, O.K. Kegyes-B, "A case study using rapid visual screening method to determine the vulnerability of

buildings in two districts of Jeddah, Saudi Arabia," *In Proceedings of the 15th International Symposium on new technologies for urban safety of megacities in Asia*, Tacloban, Philippines, Nov. 2016, pp. 7-9, [Online]. https://www.researchgate.net/publication/309736872_A_Case_Study_Using_Rapid_Visual_Screening_Method_to_Determine_the_Vulnerability_of_Buildings_in_two_Districts_of_Jeddah_Saudi_Arabia (Accessed Date: July 27, 2024).

[16] O. Kaplan, Y. Güney, A. Topçu, Y. Özçelikörs, "A rapid seismic safety assessment method for mid-rise reinforced concrete buildings," *Bulletin of Earthquake Engineering*, vol. 16, no. 2, pp. 889–915, Sep. 2017. doi: 10.1007/s10518-017-0229-0.

[17] E. Harirchian, T. Lahmer, S. Buddhiraju, K. Mohammad, A. Mosavi A, "Earthquake Safety Assessment of Buildings through Rapid Visual Screening," *Buildings*, vol. 10, no. 3, pp. 51, Mar. 2020. doi: 10.3390/buildings10030051.

[18] A. Aydin, A. Basu, "The Schmidt hammer in rock material characterization," *Engineering Geology*, vol. 81, no. 1, pp. 1–14, Sep. 2005. https://doi.org/10.1016/j.enggeo.2005.06.006.

[19] R. Surva, R. Shobana, "Design & Seismic Analysis of Single Storey 3-D Frame Using Sap2000, "*International Research Journal of Engineering and Technology (IRJET)*, vol. 18, no. 4, pp. 5582-5087, April 2021. [Online]. https://www.irjet.net/archives/V8/i4/IRJET-V8I4973.pdf (Accessed Date: July 27, 2024).

[20] M. Zameeruddin, K. Sangle, "Performance-based Seismic Assessment of Reinforced Concrete Moment Resisting Frame," *Journal of King Saud University-Engineering Sciences*, vol 33, no.3, pp. 153-165, Mar.2021. https://doi.org/10.1016/j.jksues.2020.04.005.

[21] S. Freeman, "Review of the development of the Capacity Spectrum Method," *ISET Journal of Earthquake Technology*, vol. 41, no. 1, pp. 1–13, Mar. 2004, [Online]. https://engineering.purdue.edu/~ce573/Documents/SAF_Review%20of%20Capacity%20Spectrum%20Method.pdf (Accessed Date: July 27, 2024).

[22] I.F. Moschonas, A. J. Kappos, P. Panetsos, V. Papadopoulos, T. K. Makarios, P. Thanopoulos, "Seismic fragility curves for Greek bridges: methodology and case studies," *Bulletin of Earthquake Engineering*, vol. 7, no. 2, pp. 439–468, Sep. 2008. doi: 10.1007/s10518-008-9077-2.

[23] K. R. Karim, F. Yamazaki, "A simplified method of constructing fragility curves for highway bridges," *Earthquake Engineering and Structural Dynamics/Earthquake Engineering & Structural Dynamics*, vol. 32, no. 10, pp. 1603–1626, May 2003. doi: 10.1002/eqe.291.

[24] M. Shinozuka, M. Feng, J. Lee, T. Naganuma, "Statistical Analysis of Fragility Curves," *Journal of Engineering Mechanics*, vol. 126, no. 12, pp. 1224–1231, Dec. 2000. doi: 10.1061/(ASCE)0733-9399(2000)126:12(1224).

[25] M.B. Baylon, C. S. Lictaoa, I.J.C. Castillo, C.K.P. Dungog, L.R. Jerusalem, "Seismic vulnerability assessment of Sta. Lucia high school in Pasig City Philippines using rapid visual assessment and fragility curves," *Zenodo (CERN European Organization for Nuclear Research)*, vol. 1, no. 2, pp. 119–135, Nov. 2021. doi: 10.5281/zenodo.5726470.

[26] U.Y. Vazurkar, D.J. Chaudhari, "Development of Fragility Curves for RC Buildings," *International Journal of Engineering Research*, vol. 5, no. 3, pp. 591-594, Feb. 2016, [Online]. https://www.academia.edu/27583791/Development_of_Fragility_Curves_for_RC_Buildings (Accessed Date: July 27,2024)

[27] M. Vasavada, V.R. Patel, "Development of Fragility Curves for RC Buildings using HAZUS method," *International Research Journal of Engineering and Technology (IRJET)*, vol. 3, no. 5, pp. 2256–2262, May 2016, [Online]. https://www.irjet.net/archives/V3/i5/IRJET-V3I5479.pdf (Accessed Date: July 27, 2024).

[28] T. Gehlot, S. S. Sankhla, A. Gupta, "Study of Concrete Quality Assessment of Structural Elements Using Rebound Hammer Test," *American Journal of Engineering Research (AJER)*, Vol.5, no.8, pp.192- 198, 2016, [Online]. https://www.ajer.org/papers/v5(08)/Z050801920198.pdf (Accessed Date: July 27, 2024).

[29] A. J. Pierre, "Seismic performance of reinforced concrete structures with pushover analysis," *IOP Conference Series: Earth and Environmental Science*, Indonesia, 2020, pp. 1-10. doi: 10.1088/1755-1315/426/1/012045.

[30] Y. Menasri, M. S. Nouaouria, M. Brahimi, "Probabilistic Approach to the Seismic Vulnerability of RC Frame Structures by the

Development of Analytical Fragility Curves", *International Journal of Engineering*, vol. 30, no. 7, pp. 945-954, July 2017, [Online]. https://www.ije.ir/article_72967.html (Accessed Date: July 27, 2024).

[31] A. Balingit, N. Almario, B.J. Antonio, J. Bon, J. Cada, T. J. Soriano, J.R. Gabriel, J.V. Tongol, "Seismic Assessment of Phil Health Regional Office III Building in the City of San Fernando, Pampanga, Philippines Using Fragility Curves," *International Journal of Scientific Research and Engineering Development*, vol. 7, no.3, pp.1446-1473, June 2024, [Online]. https://ijsred.com/volume7/issue3/IJSRED-V7I3P155.pdf (Accessed Date: July 27, 2024)

[32] X. Wang, C.H. Wang, Y.B. Khoo, C. Morga, M.G. Stewart, "Designing resilient structures: Mainstreaming disaster risk reduction and climate change adaptation in local design practices handbook," *Commonwealth Scientific and Industrial Research Organization (CSIRO)*, Australia, 2016, [Online]. https://philippines.embassy.gov.au/files/mnla/Designing%20Resilient%20Structures%20Handbook%202016%20(12).pdf (Accessed Date: July 27, 2024).

[33] M. J. Gemoya, R. R. Ordanez, T. Paulino, J. Razon, A. Santos, J.M. Songco, M. Tongol, J.C. Zoleta, J.R. Gabriel, M. B. Baylon, "Seismic Vulnerability Assessment of College of Engineering and Architecture (CEA) Extension Building in Don Honorio Ventura State University (DHVSU) Main Campus Using Fragility Curves", *International Journal of Progressive Research in Science and Engineering*, vol. 4, no. 6, pp. 279-286, 2023, [Online]. https://journal.ijprse.com/index.php/ijprse/article/view/917 (Accessed Date: July 27, 2024)

[34] S. A. Freeman, A. Irfanoglu, & T. F. Paret, "Earthquake engineering intensity scale: A template with many uses," *In 13th World Conference on Earthquake Engineering*, Vancouver, BC, Canada, Aug. 2004, pp. 1-15, [Online]. https://www.iitk.ac.in/nicee/wcee/article/13_1667.pdf (Accessed Date: July 27, 2024).

[35] M.B. Baylon, H. D. Caranto, A. P. Espino, B. D. Nilo, "Developing Seismic Fragility Curves of Old Hospital in Manila, Philippines," *In 3rd International Conference on Protection of Historical Constructions. Lisbon, Portugal*, 2017, pp. 1-13, [Online]. https://www.researchgate.net/publication/319187969_DEVELOPING_SEISMIC_FRAGILITY_CURVES_OF_OLD_HOSPITAL_IN_MANILA_PHILIPPINES (Accessed Date: July 24, 2024)

[36] T. Zera, M. Nafian, "Comparing Two models of mapping the peak ground acceleration (PGA) in western Java," *International Conference on Science and Technology (ICOSAT 2017)*, Jakarta, 2017, pp.140-142. DOI: 10.2991/icosat-17.2018.30.

Contribution of Individual Authors to the Creation of a Scientific Article (Ghostwriting Policy)

All authors are equal contributors to this work.

Sources of Funding for Research Presented in a Scientific Article or Scientific Article Itself

No funding was received for conducting this study.

Conflict of Interest

The authors declare that there are no conflicts of interest.

Creative Commons Attribution License 4.0 (Attribution 4.0 International, CC BY 4.0)

This article is published under the terms of the Creative Commons Attribution License 4.0
https://creativecommons.org/licenses/by/4.0/deed.en_US

APPENDIX

Table 1. Local Ground Motion Data

Location	Magnitude	Latitude	Longitude	Depth	Date
Luzon, Philippines	Mw 7.2	13.45	124.63	18.02 km	24/02/1988
Luzon, Philippines	Mw 6.5	10.81	126.83	44.4 km	17/07/1990
Mindanao, Philippines	Mw 6.5	8.33	126.52	63.2 km	25/10/1990
Samar, Philippines	Mw 7.1	12.07	125.28	20.7 km	21/04/1995
Samar, Philippines	Mw 7.0	12.63	125.58	5.3 km	05/05/1995
Philippine Islands Region	Mw 7.6	10.81	126.83	44.4 km	31/08/2012
Luzon, Philippines	Mw 7.0	17.55	120.80	46.0 km	27/07/2022

Table 2. Foreign Ground Data Motion

Location	Magnitude	Latitude	Longitude	Depth	Date
Kuril Islands	Mw 7.1	45.26	149.89	36.6 km	07/02/1996
Near the Coast of Peru	Mw 8.0	-13.38	-76.56	41.2 km	15/08/2007
Near East Coast of Japan	Mw 9.1	38.29	142.50	19.7 km	11/03/2011
Near the Coast of Central Chile	Mw 8.3	-31.57	-71.67	22.4 km	16/09/2015
Central California	Mw 7.1	35.77	-117.60	8.0 km	06/07/2019

Table 5. Summary of Compressive Strength Used for Each Building

Location of Test Area	Part of Structure	Rebound Reading Number										Average Rebound Reading	Correction Factor	Corrected Compressive Strength (MPa)
		A	B	C	D	E	F	G	H	I	J			
Engineering Building 2	**Column 1**	38.30	37.10	34.00	34.50	36.20	37.50	36.60	41.20	37.40	35.50	**36.83**	**1**	**17.80**
	Beam 1	38.10	39.30	31.30	32.70	37.10	32.80	31.20	35.50	37.30	37.80	**35.31**	**1**	**16.00**
Engineering Building 1	**Column 2**	34.60	44.10	36.80	39.20	34.90	40.00	39.90	37.00	36.70	40.50	**38.37**	**1**	**19.10**
	Beam 2	39.40	43.20	44.40	49.10	42.00	42.90	39.00	40.70	37.10	46.80	**42.46**	**1**	**21.80**
Engineering Building 3	**Column 3**	37.20	39.60	41.10	43.90	39.60	42.50	37.50	41.80	40.40	43.10	**40.67**	**1**	**21.60**
	Beam 3	41.20	42.80	3480	42.40	37.30	39.60	41.20	40.70	44.20	40.23	**40.23**	**1**	**21.30**

Table 6. Summary of the tensile strength used for each building.

Test	Engineering Building 1	Engineering Building 2	Engineering Building 3
Mechanical Properties			
Yield point (psi)	53.650	49,300	47,850
Tensile Strength (psi)	72,500	72,500	66,700
Elongation, %	20	20	20
TS/YS Ratio	1.35	1.47	1.39
Description of fracture	IRR	IRR	IRR
Bending Properties			
Degree bent, 180 degrees	No crack	No crack	No crack
Physical Properties			
Actual Unit Mass, kg/m	1.506	1.522	1.555
Variation in Mass, %	-2.96	-1.93	0.19

Table 7. Performance Points summary tabulation based on the July 16, 1990, earthquake in Luzon, Philippines (6.5)

PGA	East-West Direction				North-South Direction			
	X-Axis		Y-Axis		X-Axis		Y-Axis	
	V(KN)	D(mm)	V(KN)	D(mm)	V(KN)	D(mm)	V(KN)	D(mm)
0.1	161.629	1.013	145.137	1.238	86.033	0.560	116.230	0.846
0.2	323.265	1.981	290.276	3.203	172.059	1.075	232.456	2.420
0.3	484.893	2.948	435.413	5.168	258.092	1.590	348.686	3.994
0.4	646.522	3.916	580.549	7.133	344.124	2.106	464.910	5.567
0.5	808.158	4.884	725.688	9.097	430.157	2.621	581.142	7.141
0.6	969.787	5.852	870.825	11.062	516.183	3.136	697.366	8.714
0.7	1131.422	6.820	1015.964	13.027	602.216	3.651	813.596	10.288
0.8	1285.740	7.770	1161.101	14.992	688.249	4.166	929.820	11.861
0.9	1422.885	8.678	1306.238	16.957	774.275	4.681	1046.052	13.435
1	1559.975	9.585	1439.106	18.833	860.307	5.196	1162.286	15.008
1.1	1696.997	10.492	1538.897	20.454	946.340	5.712	1278.506	16.582
1.2	1833.959	11.399	1636.117	22.033	1032.373	6.227	1394.732	18.155
1.3	1970.866	12.305	1703.246	23.553	1118.399	6.742	1487.995	19.627
1.4	2107.706	13.211	1750.163	25.009	1204.432	7.257	1577.081	21.074
1.5	2244.484	14.117	1795.410	26.413	1285.415	7.768	1665.592	22.512
1.6	2381.208	15.022	1822.421	28.557	1362.316	8.277	1719.107	24.045
1.7	2517.866	15.927	1837.381	31.196	1439.689	8.789	1768.599	25.581
1.8	2654.468	16.831	1852.200	33.810	1517.549	9.304	1806.816	27.254
1.9	2791.004	17.735	1862.637	36.569	1595.897	9.823	1826.522	29.280
2	2914.284	18.581	1873.854	39.112	1674.729	10.345	1839.610	31.589
2.1	2954.486	19.063	1881.266	41.991	1754.063	10.870	1852.621	33.884
2.2	2993.651	19.533	1885.446	45.888	1833.898	11.399	1862.885	36.274
2.3	3027.965	20.153	1887.717	50.417	1914.238	11.931	1871.386	38.603
2.4	3048.454	21.432	1896.816	53.621	1995.082	12.466	1878.564	41.169
2.5	3068.735	22.698	1909.032	56.313	2076.447	13.004	1885.539	46.073
2.6	161.629	1.013	145.137	1.238	2158.331	13.547	1925.582	60.114
2.7	323.265	1.981	290.276	3.203	2240.735	14.092	1927.960	63.099
2.8	484.893	2.948	435.413	5.168	2323.673	14.641	1930.357	66.108
2.9	646.522	3.916	580.549	7.133	2407.149	15.194	1932.774	69.141
3.0	808.158	4.884	725.688	9.097	2491.162	15.750	1935.209	72.199

Table 8. Damage State Threshold Limits of each School Building

Building Name	X – Direction					Y – Direction				
	Spectral Displacement (mm)					Spectral Displacement (mm)				
	D	C	B	A	As	D	C	B	A	As
Engineering Building 1	0	12.892	18.417	34.585	83.088	0	11.754	16.792	33.344	83.001
Engineering Building 2	0	14.055	20.079	58.428	173.476	0	18.506	26.437	85.646	263.273
Engineering Building 3	0	33.162	47.347	103.765	272.939	0	10.348	14.783	79.024	271.748

Table 9. Sample Performance Points and Damage Ranking for Engineering Building 2 in East-West Direction (y-direction)

PGA	D (mm)	DST	PGA	D (mm)	DST
0.1	3.773	D	1.6	99.976	A
0.2	8.273	D	1.7	103.798	A
0.3	12.773	D	1.8	107.318	A
0.4	17.273	D	1.9	110.699	A
0.5	21.318	C	2	271.975	As
0.6	25.133	C	2.1	289.502	As
0.7	30.173	B	2.2	302.407	As
0.8	36.878	B	2.3	310.541	As
0.9	44.605	B	2.4	318.423	As
1.0	67.657	B	2.5	326.042	As
1.1	67.657	B	2.6	332.870	As
1.2	81.329	B	2.7	339.473	As
1.3	89.378	A	2.8	345.862	As
1.4	93.742	A	2.9	354.010	As
1.5	96.798	A	3	370.062	As

Table 10. Sample Total Number of Occurrence in the East-West Direction (y-axis) for Engineering Building 2

PGA (g)	Y - Direction					PGA (g)	Y - Direction				
	D	C	B	A	As		D	C	B	A	As
0.1	12	0	0	0	0	1.6	2	3	3	4	0
0.2	12	0	0	0	0	1.7	2	2	4	4	0
0.3	12	0	0	0	0	1.8	2	2	4	4	0
0.4	12	0	0	0	0	1.9	0	2	6	4	0
0.5	10	2	0	0	0	2.0	0	2	6	3	1
0.6	10	2	0	0	0	2.1	0	2	5	4	1
0.7	8	2	2	0	0	2.2	0	2	3	6	1
0.8	8	2	2	0	0	2.3	0	2	3	5	2
0.9	8	2	2	0	0	2.4	0	2	3	5	2
1.0	5	4	3	0	0	2.5	0	2	3	4	3
1.1	4	4	4	0	0	2.6	0	2	2	4	4
1.2	4	4	4	0	0	2.7	0	1	3	4	4
1.3	3	5	3	1	0	2.8	0	0	4	3	5
1.4	2	5	4	1	0	2.9	0	0	4	3	5
1.5	2	4	4	2	0	3.0	0	0	3	4	5

Table 11.A: Summary of Probability of Exceedance for PSU Buildings at 0.4g Peak Ground Acceleration in the East-West Direction for Each Damage Rank

Building Name	East – West							
	X – Axis				Y - Axis			
	C	B	A	As	C	B	A	As
Engineering Building 1	6.53%	5.46%	5.25%	5.23%	5.32%	5.32%	5.19%	5.44%
Engineering Building 2	5.49%	5.20%	5.22%	5.47%	7.50%	5.61%	5.20%	5.29%
Engineering Building 3	21.98%	8.07%	5.31%	5.24%	21.07%	6.84%	5.19%	5.39%

Table 11.B: Summary Of Probability of Exceedance for PSU Buildings at 0.4g peak ground acceleration in the North-South Direction for every damage rank.

Building Name	**North - South**							
	X – Axis				**Y - Axis**			
	C	**B**	**A**	**As**	**C**	**B**	**A**	**As**
Engineering Building 1	6.74%	5.38%	5.19%	5.33%	5.31%	5.25%	5.23%	0%
Engineering Building 2	5.55%	5.19%	5.21%	5.39%	6.26%	5.34%	5.34%	5.27%
Engineering Building 3	18.18%	6.54%	5.22%	5.24%	17.62%	6.82%	5.19%	5.33%

Table 12.A: Maximum Peak Ground Acceleration in the East-West Direction with a 10% Probability of Exceedance

Building Name	**East – West**							
	X – Axis				**Y - Axis**			
	C	**B**	**A**	**As**	**C**	**B**	**A**	**As**
Engineering Building 1	0.50 g	0.53 g	0.55 g	0.60 g	0.55 g	0.56 g	0.59 g	0.60 g
Engineering Building 2	0.55 g	0.58 g	0.58 g	0.60 g	0.46 g	0.53 g	0.57 g	0.60 g
Engineering Building 3	0.25 g	0.43 g	056 g	0.60 g	0.25 g	0.48 g	0.58 g	0.60 g

Table 12.B: Maximum Peak Ground Acceleration in the North-South Direction with a 10% Probability of Exceedance

Building Name	**North - South**							
	X – Axis				Y - Axis			
	C	B	A	As	C	B	A	As
Engineering Building 1	0.49 g	0.54 g	0.58 g	0.60 g	0.56 g	0.57 g	0.58 g	
Engineering Building 2	0.55 g	0.59 g	0.60 g	0.60 g	0.50 g	0.56 g	0.59 g	0.60 g
Engineering Building 3	0.29 g	0.50 g	0.58 g	0.58 g	0.29 g	0.48 g	0.58 g	0.60 g

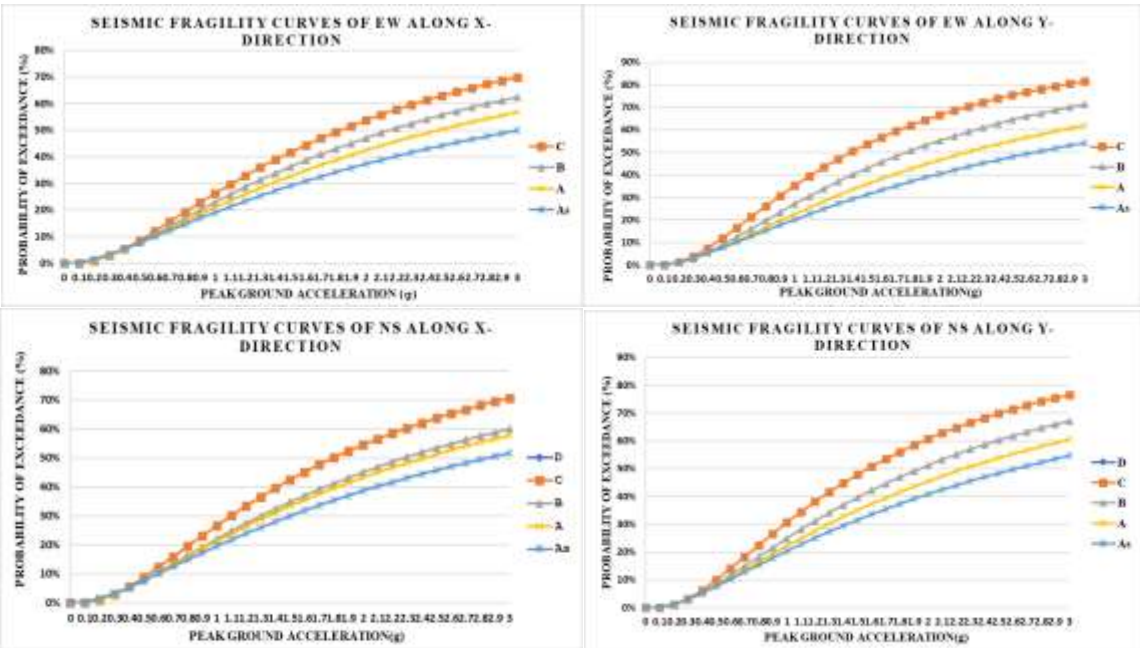

Fig. 20: Seismic Fragility Curves of Engineering Building 2

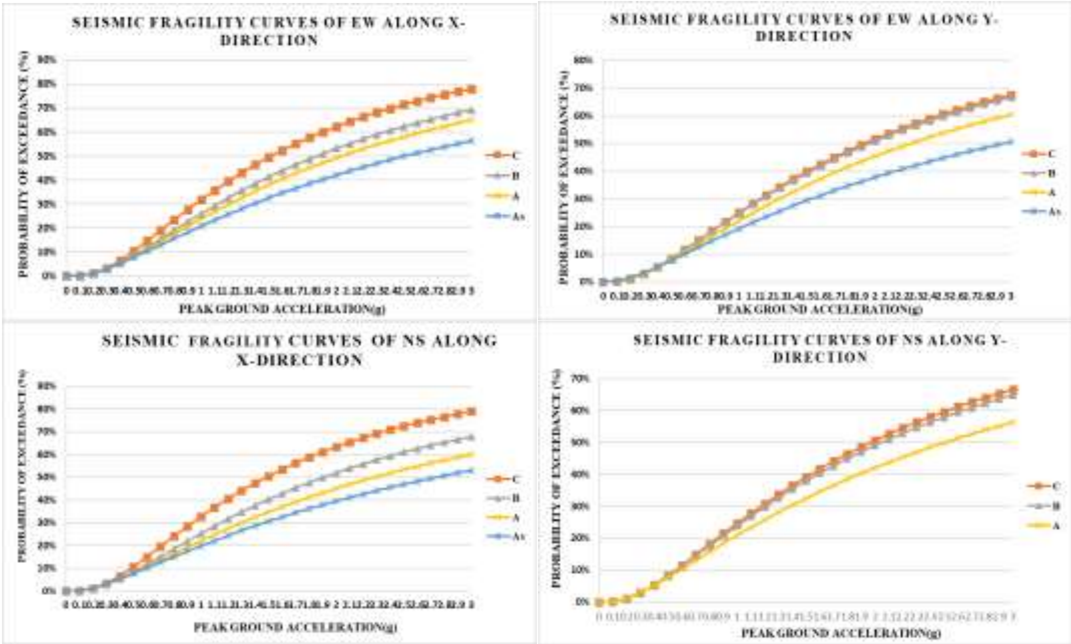

Fig. 21: Seismic Fragility Curves of Engineering Building 1

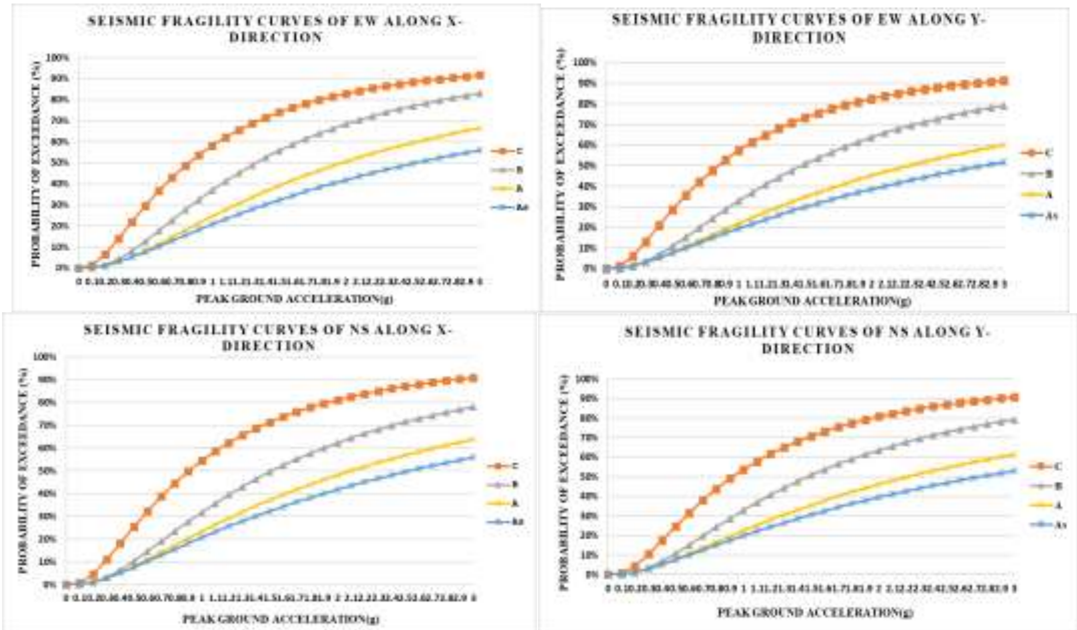

Fig. 22: Seismic Fragility Curves of Engineering Building 3